Disruption of hemocyte differentiation and distribution in Drosophila Ptr^{23c} mutants

Cristina Parada[1‡,2,3,4,5‡], María Constanza Silvera[1‡,6], Tabaré de los Campos[7], Rafael Cantera[1‡], Carmen Bolatto[5,8*], Daniel Prieto[1‡,6*]

1 Departamento de Biología del Neurodesarrollo, Instituto de Investigaciones Biológicas Clemente Estable, Uruguay.

2 Departamento de Neurofarmacología Experimental, Instituto de Investigaciones Biológicas Clemente Estable, Uruguay.

3 Unidad Académica ESFUNO, Facultad de Enfermería, Universidad de la República, Uruguay.

4 PEDECIBA - Programa de Desarrollo de las Ciencias Básicas, Uruguay.

5 Unidad Académica de Histología y Embriología, Facultad de Medicina, Universidad de la República, Uruguay.

6 Departamento de Neurofisiología Celular y Molecular, Instituto de Investigaciones Biológicas Clemente Estable, Uruguay.

7 Unidad de Electrónica, Instituto de Investigaciones Biológicas Clemente Estable, Uruguay.

8 Departamento de Neurobiología y Neuropatología, Instituto de Investigaciones Biológicas Clemente Estable, Uruguay.

‡ Past Affiliation

* Corresponding author

Abstract

In *Drosophila*, hemocytes are essential for development and immunity, with their differentiation and spatial distribution under strict regulation. Here, we examine the effect of the *Ptr^{23c}* null mutation in embryonic hemocyte development. Contrary to our initial hypothesis, *Ptr* does not regulate hemocyte number, as the mutation did not affect the total number of hemocytes, apoptosis, mitosis, or the balance between major subpopulations. However, *Ptr^{23c}* mutants displayed disrupted distribution and premature hemocyte differentiation, marked by accelerated maturation at stage 12. Despite this early differentiation, *Ptr^{23c}* embryos exhibited a 50% reduction in mature hemocytes by stage 16, as quantified by *serpent*-driven mCherry expression. Our findings establish Ptr as a regulator of hemocyte distribution and differentiation timing during normal embryogenesis, possibly through modulation of the *serpent* pathway.

Introduction

Patched-related (Ptr) is a conserved transmembrane protein belonging to the patched domain-containing protein family (Kuwabara and Labouesse, 2002; Pastenes et al., 2008). In *Drosophila melanogaster*, Ptr can interact directly with the signaling protein Hedgehog (Hh) and *Ptr*[23c] null mutants exhibit phenotypic defects similar to those observed in Hh pathway mutants (Bolatto et al., 2022). Furthermore, cell culture assays suggest that Ptr acts as a negative regulator of Hh signaling (Bolatto et al., 2015, 2022).

Ptr is expressed in hemocytes (Bolatto et al., 2015; Cattenoz et al., 2020), which are arthropod blood cells, though its precise role in these cells remains unclear. Hemocytes are essential for immunity and development, with *Drosophila* possessing three main subtypes: plasmatocytes, crystal cells (CCs), and lamellocytes (Honti et al., 2014; Nappi and Vass, 1993; Yu et al., 2022). During *Drosophila* development plasmatocytes are, by far, the most common type of hemocyte. Constituting around 95% of circulating hemocytes, they function as phagocytes, bearing similarities to mammalian macrophages and monocytes (Gold and Brückner, 2015; Meister, 2004; Yoon et al., 2023). These migratory cells are responsible for phagocytizing apoptotic cells, tumor cells and invading microorganisms. They recycle the nutrients from the material that they have ingested and secrete antimicrobial peptides and components of the extracellular matrix (Evans and Wood, 2014; Krejčová et al., 2024; Wang et al., 2014).

Due to evolutionary conservation in hematopoiesis (Evans et al., 2003; Gold and Brückner, 2015; Lebestky et al., 2000), *Drosophila* hemocytes serve as a model for studying immune responses, tissue remodeling, wound healing, and even metastasis (McDonald and Montell, 2004; Yoon et al., 2023).

Embryonic hemocytes originate from procephalic mesodermal derivatives beginning from stage 8 onwards. At this stage, a population of mesodermal precursors undergoes four rounds of mitosis and reach a total of 600-700 cells (Tepass et al., 1994; Gyoergy et al., 2018). These numbers remain stable until the end of embryonic development (Vlisidou and Wood, 2015).

During germ-band extension hemocytes colonize the head region before migrating across the epithelial barrier between the head and tail (Tepass et al., 1994; de Velasco et al., 2006; Siekhaus et al., 2010). They then disperse along three stereotyped migratory paths: the ventral

midline (dorsal and ventral to the developing ventral nerve cord), the intestinal primordium, and beneath the epidermis, along the developing dorsal vessel (Cho et al.; 2002 Ratheesh et al., 2015). As they migrate, hemocytes deposit extracellular matrix components and engulf cell debris resulting from developmental apoptosis (Tepass et al., 1994; Sonnenfeld and Jacobs, 1995; Manaka et al., 2004).

By stage 15 of embryogenesis, the hemocytes are evenly dispersed throughout the embryo, yet they still have the capacity to migrate to wound sites (Fauvarque and Williams, 2011; Moreira et al., 2011; Ratheesh et al., 2015; Tepass et al., 1994). Targeted ablation of hemocytes results in elevated embryonic lethality and defects in the ventral nerve cord (Defaye et al., 2009), as well as pupal lethality (Matsubayashi et al., 2017; Stephenson et al., 2022).

Our previous research revealed that late Ptr^{23c} embryos have reduced hatching ability (Bolatto et al., 2022; Parada and Prieto, 2025), which might explain their substantial embryonic lethality (Bolatto et al., 2015). Increased mortality was also observed at subsequent developmental stages (Parada and Prieto, 2025) and an apparent reduction in the number of embryonic hemocyte has been suggested (Bolatto et al., 2015). Given the fundamental role of hemocytes in embryonic development, a decrease in their number could potentially contribute to the reduced viability of Ptr^{23c} embryos and larvae. In this study, we investigate the effect of Ptr^{23c} mutation in the number, proliferation, apoptosis and distribution of hemocytes during embryogenesis. The specific mechanisms affected in Ptr^{23c} mutants remain unknown.

Materials and Methods

Genetics and Drosophila strains

srpHemo-H2A::3xmCherry was kindly gifted by Dr. Daria Siekhaus (Gyoergy et al., 2018). This stock was used to generate both the control strain (+/+, *twi-GFP*; *srpHemo-H2A::3xmCherry/srpHemo-H2A::3xmCherry*) and the Ptr^{23c}/*CyO, twi-GFP*; *srpHemo-H2A::3xmCherry/srpHemo-H2A::3xmCherry* strain. Flies were maintained on a standard cornmeal, yeast and glucose medium at 25°C with 12h-dark and light cycles.

Embryo collection and fixation

Flies were allowed to lay eggs on apple-juice agar plates supplemented with yeast. The eggs were collected, rinsed with water, dechorionated in 5% sodium hypochlorite and washed with PBST (0.05% Triton X-100 in phosphate-buffered saline). The embryos were then fixed by shaking them in a 1:1 mixture of heptane and 4% paraformaldehyde (PFA) for 20 minutes. The vitelline membrane was removed by replacing the PFA with cold methanol (-20°C) and shaking for 1 minute. The fixed embryos were then stored in fresh methanol at -20°C until further use.

Immunofluorescence

The embryos were rehydrated and incubated with PBST 3% BSA for 1 hour. Immunostaining was performed using the following antibodies: rabbit anti-phosphorylated Histone H3 (1:200, Cell Signaling Technologies #9713), rat anti-mCherry (1:500, Invitrogen #M11217) or rabbit anti-Dcp-1 (cleaved *Drosophila* Death caspase-1) (1:100, Cell Signaling Technologies #9578). The embryos were then incubated with the antibodies at 4°C overnight, washed with PBST and incubated for 2 hours with the following fluorescently conjugated antibodies goat anti-rat (1:500, Invitrogen, A11011), goat anti-rabbit (1:500, Invitrogen #A11034) or Alexa Fluor 647-conjugated Peanut Agglutinin (PNA, 10 mg/ml, Molecular Probes #L-32460). After washing with PBS, the embryos were mounted in 80% Tris-buffered glycerol.

Microscopy, Quantification and Statistical Analysis

Confocal images were acquired using a Zeiss LSM800 laser-scanning confocal microscope using either an EC Plan-Neofluar 20x/0.50 or a Plan-Apochromat 63x/1.40 M27 objective with GaAsP-PMT and Multialkali detectors. Images were analyzed using FIJI for Linux (Schindelin et al., 2012).

To calculate the mitotic index, stacks of confocal images taken along the longitudinal axis of vertically mounted embryos were processed and quantified using Object Counter 3D. Double-stained nuclei were identified in a new stack generated from the original channels in Image calculator using the logical operator 'AND', followed by Object Counter 3D particle analysis excluding sizes under 5 μm^3.

To quantify the total number of hemocyte and apoptotic hemocytes, embryos were mounted between two coverslips and z-stacks of confocal images were obtained orthogonally to the longitudinal body axis were obtained for every half embryo. Whole embryos were reconstructed in three dimensions with FIJI, and quantification was performed using Object Counter 3D particle analysis.

A FIJI/ImageJ macro was developed specifically for analyzing hemocyte distribution. The perimeter of the embryo was determined using PNA staining and divided into 19 equally spaced concentric regions of interest (ROIs). We measured mCherry integrated density within each ROI. Each value was then expressed as a percentage of the total for each embryo. Data analysis was performed using either GraphPad Prism (version 6.01 for Windows, GraphPad Software, San Diego, CA, USA, www.graphpad.com) or R/Bioconductor 4.4.1.

Flow Cytometry

A pool of 150 dechorionated embryos was disaggregated in HL solution (Salmand et al., 2011) using a Dounce homogenizer. The mixture was then filtered through a 100 μm mesh and centrifuged at 400 g for 5 min. The pellet was then resuspended in HL containing 2 mM EDTA and filtered through a 40 μm mesh. The cells were then fixed for 10 min in 4% PFA, washed in PBST, acquired using an Attune™ NxT cytometer, and analyzed in R/Bioconductor 4.4.1 based on a previously described method (Gonzalez et al., 2023). The fluorescence emitted by the mCherry reporter in hemocytes at three embryonic stages was quantified to obtain a discrete time series for the Ptr^{23c} strain and the control strain.

Results

Quantification of hemocyte number and death

Based on preliminary data, it was suggested that the Ptr^{23c} null mutation reduces the number of hemocytes in *Drosophila* embryos (Bolatto et al., 2015). To investigate this possibility, we introduced a hemocyte-specific nuclear mCherry reporter into the Ptr^{23c} strain to enable the identification of individual hemocytes (Gyorgey et al., 2018). Confocal microscopy stacks were used to count all hemocytes in each embryo examined at the onset of stage 16 (Figure 1A). In

the control sample, we found the median count was around 600 cells (Figure 1B), which is consistent within the counts obtained using both the same methodology (Gyoergy et al., 2018) and a different methodology (Tepass et al., 1994). The same result was obtained when examining the Ptr^{23c} mutant samples. The median hemocyte count was 601 for control embryos (n = 15) and 618 for Ptr^{23c} embryos (n = 14) (Figure 1B).

Having observed that the mutation did not appear to alter the total number of hemocytes present at stage 16, we investigated whether it caused a shift in the relative proportions of the two major hemocyte populations in the embryo, plasmatocytes and CCs. At stage 16, CCs can easily identified from other hemocytes because they remain clustered around the proventriculus and possess large nuclei (Lebestky et al., 2000). Interestingly, we observed no significant difference in the number of CCs in Ptr^{23c} embryos (median = 41, n = 11) compared to controls (median = 45, n = 11) (Figure 1C).

In order to investigate whether the Ptr^{23c} mutation increases apoptosis among embryonic hemocytes, we counted the number of particles that were positive for both the hemocyte marker srpHemo-H2A::3XmCherry and the apoptotic marker Dcp-1 (see Figure 1A and A'). Stage 16 was chosen for this analysis since Ptr expression in hemocytes of a wild-type strain has been demonstrated at this stage (Bolatto et al., 2015; Cattenoz et al., 2020), and our initial observation of an apparent reduction in Ptr^{23c} hemocyte numbers was made at this stage (Bolatto et al., 2015). No differences were detected in the number of apoptotic hemocytes (Ptr^{23c} median = 25.5, n = 14; control median = 27, n = 16; see Figure 1D) or in total apoptosis (data not shown).
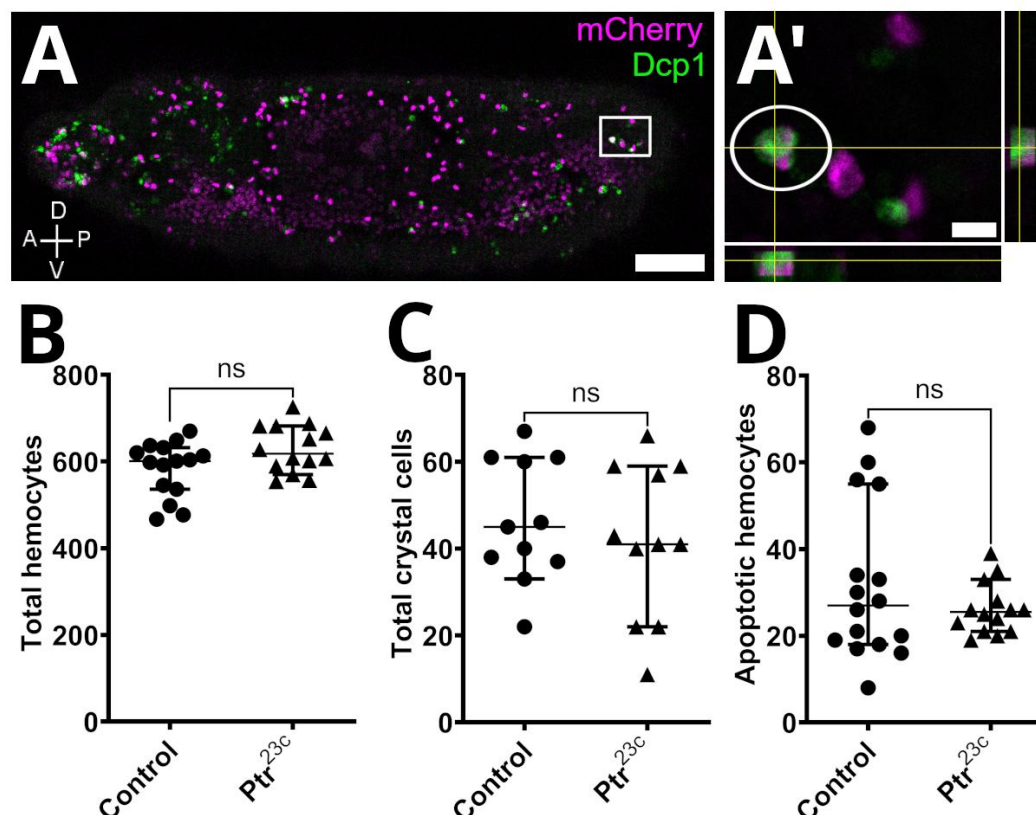
Figure 1. Hemocyte number, death, and distribution at stage 16 in *Ptr^23c* embryos. (A and A') Embryonic hemocytes, which express the nuclear marker mCherry (*srpHemo-H2A::3XmCherry*), were immunostained using anti-Dcp-1 (cleaved *Drosophila* Death caspase 1). (A) Apoptotic hemocytes were defined by the colocalization of the apoptotic marker and the hemocyte-specific nuclear mCherry signal (white circle). (A') Orthogonal optical planes are shown. The number of (B) total hemocytes, (C) total crystal cells and (D) apoptotic hemocytes were counted in embryos of each genotype. Scale bars: (A) 50 µm; (A') 5 µm.

Hemocyte distribution

As the *Ptr^23c* mutation did not affect the total number of hemocytes, we investigated whether an altered distribution pattern at stage 16 could explain the previous observation of fewer number of hemocytes in the ventral region of *Ptr^23c* embryos (Bolatto et al., 2015). To this end we developed a FIJI/ImageJ macro that defined concentric bands as regions of interest (ROIs) ranging from the periphery (ring 1) to the center (ring 19) of the embryo (n=15) (see

Figure 2A, left panel). Notably, we found a significant difference in hemocyte distribution between Ptr^{23c} and control embryos (W= 53371, p= 8.6x10^{-11}, Wilcoxon rank sum test with continuity correction) (Figure 2B). Hemocytes were less abundant at the periphery and center of the Ptr^{23c} embryos relative than in controls, with significant differences (p < 0.05, Wilcoxon U-test) observed in rings 1, 2, 17, 18, and 19 (Figure 2B).
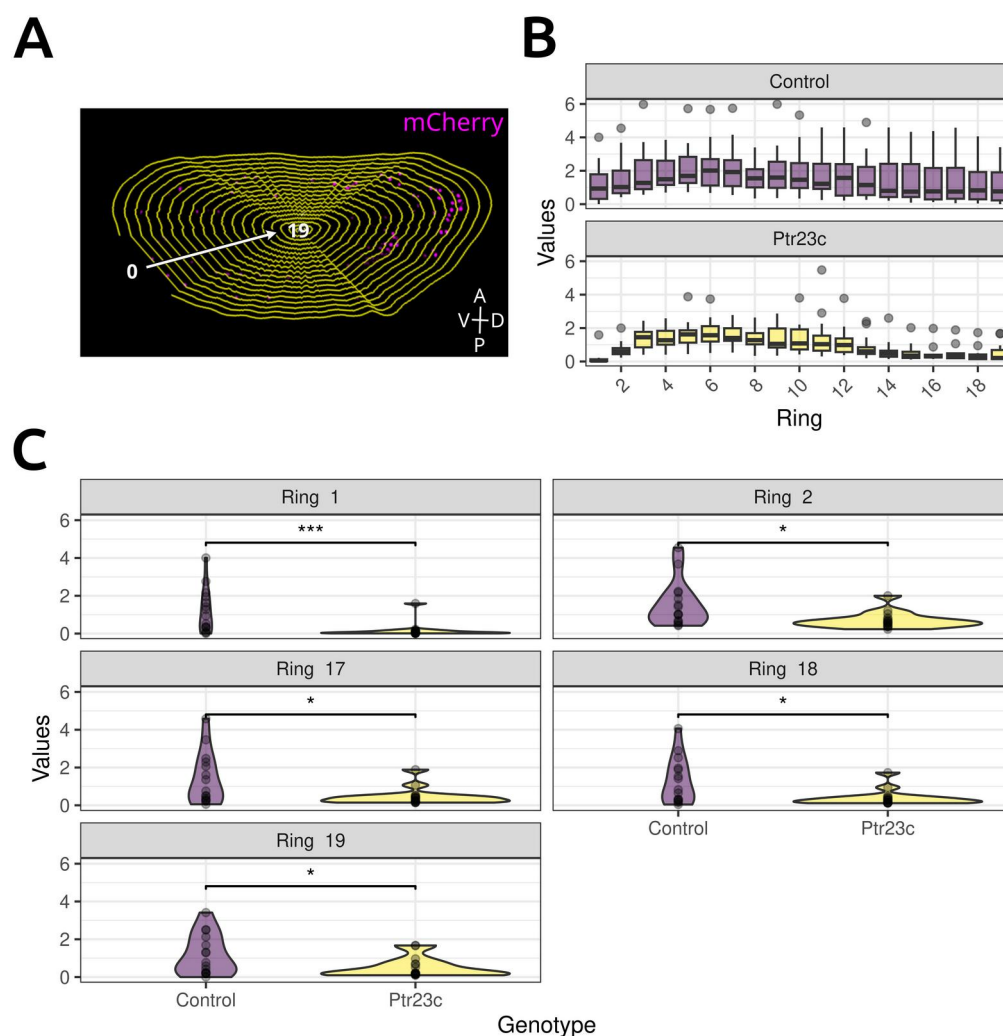

Figure 2. Hemocyte distribution at stage 16 in Ptr^{23c} embryos. (A) Integrated density of mCherry fluorescence detected in 19 concentric rings, defined as regions of interest (ROIs) numbered from the periphery (ring1) towards the center (ring 19). The two genotypes exhibited statistically different distributions (W = 53371, p = 8.613e-11, Wilcoxon rank sum test with continuity correction). (B) Rings with statistically significant differences are shown (rings 1, 2, 17, 18 and 19, Wilcoxon U-test, p<0.05). N = 15.

Hemocyte proliferation and differentiation

Mitosis among embryonic hemocytes typically stops at stage 11 (Tepass et al., 1994). To investigate whether the observed hemocytes distribution at stage 16 in Ptr^{23c} mutants was the result of delayed early proliferation, we counted mitotic hemocytes at stage 10 using immunolabeling of mitotic mCherry-positive cells with antibodies against phosphorylated histone H3 (anti-PH3) (see Figure 3A). No statistical difference in the mitotic index was detected between Ptr^{23c} (median = 0.039, n = 8) and control (median = 0.011, n = 7) embryos at this stage (Figure 3B).

Flow cytometry analysis at stage 12, using *srp*Hemo-H2A::mCherry fluorescence as an indicator of differentiation, revealed that the fluorescence intensity of *srpHemo-H2A::mCherry*-positive hemocytes was 73.5% higher in Ptr^{23c} embryos (5.9%) than in controls (3.4%) (Figure 3C). This suggests that hemocytes in Ptr^{23c} embryos exhibit elevated *serpent* (*srp*) expression at stage 12.

By stage 14, both Ptr^{23c} and control embryos showed similar percentages of hemocytes with higher intensity *srpHemo*-H2A::mCherry fluorescence. This convergence suggests that hemocyte *srp* expression had stabilized by this stage (Figure 3D).

At stage 16, hemocytes reached their highest mCherry signal. However, Ptr^{23c} embryos exhibited 50% fewer hemocytes with high-intensity-fluorescence (3%) than controls (4.5%) (Figure 3E). Altered expression of the hemocyte differentiation marker *srp* could have significant implications for immune function and developmental viability (Shlyakhover et al., 2018; Bazzi et al., 2018; Monticelli et al., 2024).
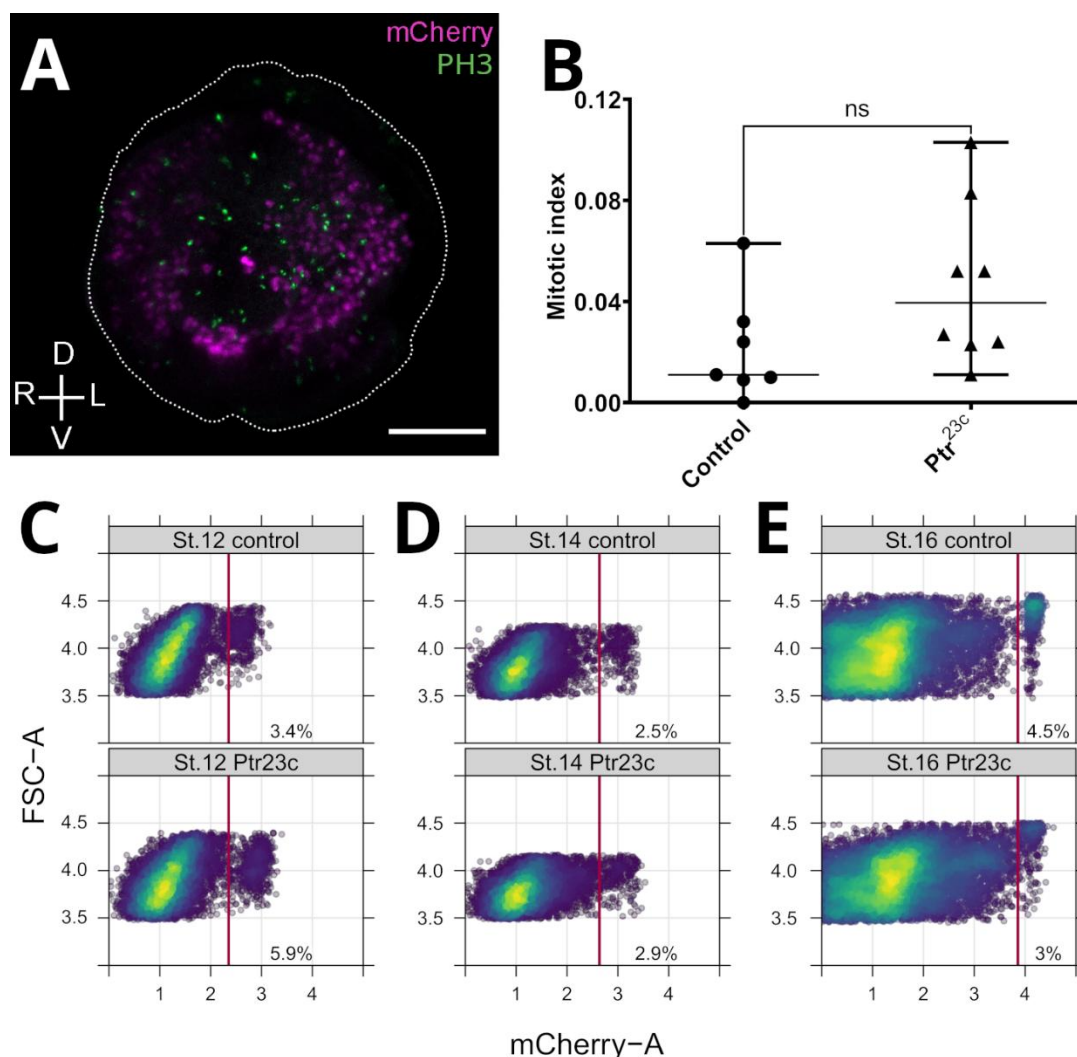
Figure 3. *Ptr^{23c}* mutants show a normal mitotic index and altered differentiation pattern in embryonic hemocytes. (A) Stage 10 embryos expressing nuclear mCherry were immunostained with an anti-PH3 antibody. The cephalic region of the embryo was imaged using confocal laser microscopy. (B) The number of double-positive nuclei was determined and the mitotic index was calculated. The medians were 0.0110 (control) and 0.0395 (*Ptr^{23c}*) (Mann-Whitney U-test). (C-E) Time course of hemocyte differentiation in *Ptr^{23c}* mutants. Flow cytometry analysis of hemocyte population (*srp*::mCherry+ cells). (C) Based on cytometric evaluation of mCherry reporter fluorescence, a subset of hemocytes with higher fluorescence intensity was quantified. At stage 12 a greater number of hemocytes with high reporter expression were observed in *Ptr^{23c}* embryos than in control embryos. This represented a higher percentage (5.9%) of the total number of cells within the Non Debris/Singlets gate than in the control group (3.4%). (D) At stage 14, mCherry fluorescence increased in embryos, and the

percentage difference between Ptr^{23c} hemocytes (2.9%) and control hemocytes (2.5%) decreased. (E) At stage 16, shortly after dispersal, hemocytes exhibited a peak in mCherry fluorescence and the percentage difference had reverted. Putative mature hemocytes from Ptr^{23c} embryos were 50% (3%) lower than in the control group (4.5%). N = 150. Scale bar: 50 µm. L: left, R: right, D: dorsal, V: ventral.

Discussion

In this study, we explored the impact of a null mutation (Ptr^{23c}) of the gene Ptr in the regulation of the embryonic $Drosophila$ hemocytes development. Our results suggest that Ptr^{23c} leads to significant disruptions in hemocyte distribution and the timing of differentiation, which could potentially affect the development of other tissues and immune processes (Bazzi et al., 2018; Monticelli et al., 2024).

Initially we hypothesized that Ptr^{23c} reduced the total number of hemocytes, because we had observed a decrease in hemocyte numbers in the ventral region of Ptr^{23c} mutant embryos at stage 16 (Bolatto et al., 2015). However, the present analysis, which is far more systematic and quantitative, revealed no significant differences in hemocyte counts. Similarly, the reduction in hemocytes could also not be explained by a shift in subpopulations towards CC differentiation. Interestingly, we also observed changes in the spatial distribution of hemocytes, specifically a reduction in their abundance in the peripheral and central regions of the Ptr^{23c} mutant embryo. This may explain the lower number of hemocytes previously observed in the ventral region (Bolatto et al., 2015).

Defects in hemocyte migration, as observed in pvr mutants, have been described to be associated with subsequent high hemocyte death by apoptosis (Brückner et al., 2004). Our quantification of the total number of apoptotic cells and of apoptotic hemocytes in Ptr^{23c} embryos revealed no increase relative to control embryos. This suggests the altered hemocyte distribution in the mutant was not due to cell loss or apoptosis-driven migration.

Interestingly, a reduction in the number of Repo-positive glia was observed in Ptr^{23c} embryos (Bolatto et al., 2022). This feature is also present in *repo* mutants, where reduced clearance of apoptotic bodies by phagocytic glia leads to secondary hemocyte recruitment. This represents a compensatory mechanism that counteracts glial loss by attracting hemocytes to the ventral nerve cord without altering the total hemocytes count (Armitage et al., 2020). Similarly, the changes in hemocyte distribution observed in Ptr^{23c} embryos may suggest a broader and homogeneous compensatory response to potential alterations in other developing tissues. This is consistent with our previous report of muscular defects in Ptr^{23c} larvae (Parada et al., 2025).

The hemocyte marker *srp*Hemo-H2A::3XmCherry not only allowed us to specifically detect hemocyte nuclei (Gyoergy et al., 2018) and the time at which the endogenous gene was switched on. Our flow cytometry analysis showed evident changes in the expression of the *srp*-directed fluorescent reporter in the Ptr^{23c} mutant, indicating an early onset or an accelerated differentiation of hemocytes. Srp is also required in the larval lymph gland during embryonic hematopoiesis, where it is necessary and sufficient to induce hemocyte development (Spahn et al., 2014). This suggests that the Ptr^{23c} mutation might accelerate the transition from progenitor cells to differentiated hemocytes.

Srp induces hemocyte differentiation by regulating the expression of phagocytic receptors (Shlyakhover et al., 2018), and the resulting plasmatocyte-mediated phagocytosis induces their own maturation (Weavers et al., 2016). Following their embryonic dispersal, hemocytes differentiate into mature cells while downregulating *srp* expression (Rehorn et al., 1996). The mechanisms governing this downregulation are not yet fully understood, but our observations suggest that the early differentiation of mCherry+ hemocytes in Ptr^{23c} mutants may cause premature *srp* downregulation. This could explain the reduced number of mCherry+ (and therefore probably mature) hemocytes observed in Ptr^{23c} mutants by stage 16. While a clear departure from the normal *srp* expression pattern is evident in the absence of *Ptr*, it would be desirable to further investigate this issue by using additional differentiation markers. Although early differentiation could affect hemocyte maturation, the observed changes in the

distribution could be explained by compensatory mechanisms due to a reduced number of glial cells.

The molecular mechanisms underlying the premature differentiation of hemocytes in Ptr^{23c} mutants remain unclear. In the larva, hemocyte progenitors are kept quiescent or undifferentiated through via Hedgehog-Patched signaling (Csordás et al., 2021; Hultmark and Andó, 2022; Mandal et al., 2007; Tokusumi et al., 2018), which is activated by Srp (Tokusumi et al., 2010). Previous evidence suggested that Ptr acts as a negative regulator of the Hh pathway (Bolatto et al., 2022). Therefore, it is possible that Ptr affects other relevant signaling pathways through Hh signalling, such as those involving Notch or autophagy, which are known to regulate hemocyte differentiation and migration (Katz et al., 2024; Leitão and Sucena, 2015). Further investigation of these pathways is necessary to better understand how Ptr modulates hemocyte dynamics.

Our findings integrate Ptr into the complex signaling network governing hemocyte development in $Drosophila$. Analysis of the Ptr^{23c} mutant phenotype demonstrates that Ptr plays a key role in regulating hemocyte differentiation and spatial distribution.
In summary, our study identifies Ptr as a relevant factor in embryonic hemocyte development. Future studies should explore the precise molecular mechanisms by which Ptr influences hemocyte dynamics, as well as the broader consequences of the lack of Ptr deficiency on immune function and organismal development.

Acknowledgements

References

Armitage, E.L., Roddie, H.G., Evans, I.R., 2020. Overexposure to apoptosis via disrupted glial specification perturbs *Drosophila* macrophage function and reveals roles of the CNS during injury. Cell Death Dis 11, 627. https://doi.org/10.1038/s41419-020-02875-2

Bazzi, W., Cattenoz, P.B., Delaporte, C., Dasari, V., Sakr, R., Yuasa, Y., Giangrande, A., 2018. Embryonic hematopoiesis modulates the inflammatory response and larval hematopoiesis in *Drosophila*. eLife 7, e34890. https://doi.org/10.7554/eLife.34890

Bolatto, C., Nieves, S., Reyes, A., Olivera-Bravo, S., Cambiazo, V., 2022. Patched-related is required for proper development of embryonic *Drosophila* nervous system. Front. Neurosci. 16, 920670. https://doi.org/10.3389/fnins.2022.920670

Bolatto, C., Parada, C., Revello, F., Zuñiga, A., Cabrera, P., Cambiazo, V., 2015. Spatial and temporal distribution of Patched-related protein in the *Drosophila* embryo. Gene Expr. Patterns 19, 120–128. https://doi.org/10.1016/j.gep.2015.10.002

Brückner, K., Kockel, L., Duchek, P., Luque, C.M., Rørth, P., Perrimon, N., 2004. The PDGF/VEGF receptor controls blood cell survival in *Drosophila*. Dev. Cell 7, 73–84. https://doi.org/10.1016/j.devcel.2004.06.007

Cattenoz, P.B., Sakr, R., Pavlidaki, A., Delaporte, C., Riba, A., Molina, N., Hariharan, N., Mukherjee, T., Giangrande, A., 2020. Temporal specificity and heterogeneity of *Drosophila* immune cells. EMBO J 39. https://doi.org/10.15252/embj.2020104486

Cho, N.K., Keyes, L., Johnson, E., Heller, J., Ryner, L., Karim, F., Krasnow, M.A., 2002. Developmental Control of Blood Cell Migration by the Drosophila VEGF Pathway. Cell 108, 865–876. https://doi.org/10.1016/S0092-8674(02)00676-1

Csordás, G., Gábor, E., Honti, V., 2021. There and back again: The mechanisms of differentiation and transdifferentiation in *Drosophila* blood cells. Dev Biol 469, 135–143. https://doi.org/10.1016/j.ydbio.2020.10.006

De Velasco, B., Mandal, L., Mkrtchyan, M., Hartenstein, V., 2006. Subdivision and developmental fate of the head mesoderm in *Drosophila* melanogaster. Dev Genes Evol 216, 39–51. https://doi.org/10.1007/s00427-005-0029-4

Defaye, A., Evans, I., Crozatier, M., Wood, W., Lemaitre, B., Leulier, F., 2009. Genetic ablation of *Drosophila* phagocytes reveals their contribution to both development and resistance to bacterial Infection. J Innate Immun 1, 322–334. https://doi.org/10.1159/000210264

Evans, C.J., Hartenstein, V., Banerjee, U., 2003. Thicker than blood. Dev Cell 5, 673–690. https://doi.org/10.1016/S1534-5807(03)00335-6

Evans, I.R., Wood, W., 2014. *Drosophila* blood cell chemotaxis. Curr. Opin. Cell Biol. 30, 1–8. https://doi.org/10.1016/j.ceb.2014.04.002

Fauvarque, M.-O., Williams, M.J., 2011. *Drosophila* cellular immunity: a story of migration and adhesion. J. Cell Sci. 124, 1373–1382. https://doi.org/10.1242/jcs.064592

Gold, K.S., Brückner, K., 2015. Macrophages and cellular immunity in *Drosophila melanogaster*. Semin. Immunol. 27, 357–368. https://doi.org/10.1016/j.smim.2016.03.010

Gonzalez, A.C., Abreu, C., Pantano, S., Comini, M., Malacrida, L., Egger, B., Cantera, R., Prieto, D., 2023. A FRET-based cGMP biosensor in *Drosophila*. MicroPubl. Biol. 2023. https://doi.org/10.17912/micropub.biology.000887

Gyoergy, A., Roblek, M., Ratheesh, A., Valoskova, K., Belyaeva, V., Wachner, S., Matsubayashi, Y., Sánchez-Sánchez, B.J., Stramer, B., Siekhaus, D.E., 2018. Tools allowing independent visualization and genetic manipulation of *Drosophila melanogaster* macrophages and surrounding tissues. G3 (Bethesda) 8, 845–857. https://doi.org/10.1534/g3.117.300452

Honti, V., Csordás, G., Kurucz, É., Márkus, R., Andó, I., 2014. The cell-mediated immunity of *Drosophila* melanogaster: Hemocyte lineages, immune compartments, microanatomy and regulation. Dev. Comp. Immunol. 42, 47–56. https://doi.org/10.1016/j.dci.2013.06.005

Hosoya, T., Takizawa, K., Nitta, K., Hotta, Y., 1995. glial cells missing: a binary switch between neuronal and glial determination in *Drosophila*. Cell, 82(6), 1025–1036. https://doi.org/10.1016/0092-8674(95)90281-3

Hultmark, D., Andó, I., 2022. Hematopoietic plasticity mapped in *Drosophila* and other insects. eLife 11, e78906. https://doi.org/10.7554/eLife.78906

Katz, M.J., Rodríguez, F., Evangelisti, F., Perez-Pandolfo, S., Sommario, N., Borrat, A., Melani, M., Wappner, P., 2024. Autophagy controls differentiation of *Drosophila* blood cells by regulating Notch levels in response to nutrient availability. https://doi.org/10.1101/2024.06.25.600418

Krejčová, G., Danielová, A., Sehadová, H., Dyčka, F., Kubásek, J., Moos, M., Bajgar, A., 2024. Macrophages play a nutritive role in post-metamorphic maturation in *Drosophila*. Development 151, dev202492. https://doi.org/10.1242/dev.202492

Kuwabara, P.E., Labouesse, M., 2002. The sterol-sensing domain: multiple families, a unique role? Trends Genet. 18, 193–201. https://doi.org/10.1016/S0168-9525(02)02640-9

Lebestky, T., Chang, T., Hartenstein, V., Banerjee, U., 2000. Specification of *Drosophila* Hematopoietic Lineage by Conserved Transcription Factors. Science 288, 146–149. https://doi.org/10.1126/science.288.5463.146

Leitão, A.B., Sucena, É., 2015. *Drosophila* sessile hemocyte clusters are true hematopoietic tissues that regulate larval blood cell differentiation. eLife 4, e06166. https://doi.org/10.7554/eLife.06166

Manaka, J., Kuraishi, T., Shiratsuchi, A., Nakai, Y., Higashida, H., Henson, P., Nakanishi, Y., 2004. Draper-mediated and phosphatidylserine-independent phagocytosis of apoptotic cells by *Drosophila* hemocytes/macrophages. J. Biol. Chem. 279, 48466–48476. https://doi.org/10.1074/jbc.M408597200

Mandal, L., Martinez-Agosto, J.A., Evans, C.J., Hartenstein, V., Banerjee, U., 2007. A Hedgehog-and Antennapedia-dependent niche maintains *Drosophila* haematopoietic precursors. Nature 446, 320–324. https://doi.org/10.1038/nature05585

Matsubayashi, Y., Louani, A., Dragu, A., Sánchez-Sánchez, B.J., Serna-Morales, E., Yolland, L., Gyoergy, A., Vizcay, G., Fleck, R.A., Heddleston, J.M., Chew, T.-L., Siekhaus, D.E., Stramer, B.M., 2017. A moving source of matrix components is essential for de novo basement

membrane formation. Curr. Biol. 27, 3526-3534.e4. https://doi.org/10.1016/j.cub.2017.10.001

McDonald, J.A., Montell, D.J., 2004. Analysis of cell migration using *Drosophila* as a model system, in: cell migration. Methods Mol Biol. Humana Press, pp. 175–202. https://doi.org/10.1385/1-59259-860-9:175

Meister, M., 2004. Blood cells of *Drosophila*: cell lineages and role in host defense. Curr. Opin. in Immunol. 16, 10–15. https://doi.org/10.1016/j.coi.2003.11.002

Monticelli, S., Sommer, A., AlHajj Hassan, Z., Garcia Rodriguez, C., Adé, K., Cattenoz, P., Delaporte, C., Gomez Perdiguero, E., Giangrande, A., 2024. Early-wave macrophages control late hematopoiesis. Dev. cell, *59*(10), 1284–1301.e8. https://doi.org/10.1016/j.devcel.2024.03.013

Moreira, C.G.A., Regan, J.C., Zaidman-Rémy, A., Jacinto, A., Prag, S., 2011. *Drosophila* hemocyte migration: an in vivo assay for directional cell migration, in: Wells, C.M., Parsons, M. (Eds.), Cell Migration, Methods Mol. Biol. Humana Press, Totowa, NJ, pp. 249–260. https://doi.org/10.1007/978-1-61779-207-6_17

Nappi, A.J., Vass, E., 1993. Melanogenesis and the generation of cytotoxic molecules during insect cellular immune reactions. Pigment Cell Res. 6, 117–126. https://doi.org/10.1111/j.1600-0749.1993.tb00590.x

Parada, C., & Prieto, D., 2025. Survival, Movement, and Lifespan: Decoding the Roles of Patched-Related in *Drosophila melanogaster*. Arch. Insect Biochem. Physiol. 118(3), e70048. https://doi.org/10.1002/arch.70048

Pastenes, L., Ibáñez, F., Bolatto, C., Pavéz, L., Cambiazo, V., 2008. Molecular characterization of a novel patched-related protein in *Apis mellifera* and *Drosophila melanogaster*. Arch. Insect Biochem. Physiol. 68, 156–170. https://doi.org/10.1002/arch.20245

Ratheesh, A., Belyaeva, V., Siekhaus, D.E., 2015. *Drosophila* immune cell migration and adhesion during embryonic development and larval immune responses. Curr. Opin. Cell Biol. 36, 71–79. https://doi.org/10.1016/j.ceb.2015.07.003

Rehorn, K. P., Thelen, H., Michelson, A. M., Reuter, R. 1996. A molecular aspect of hematopoiesis and endoderm development common to vertebrates and

Drosophila. Development (Cambridge, England), 122(12), 4023–4031. https://doi.org/10.1242/dev.122.12.4023

Rizki, M.T.M., Rizki, R.M., 1959. Functional significance of the crystal cells in the larva of *Drosophila melanogaster*. J. Cell Biol. 5, 235–240. https://doi.org/10.1083/jcb.5.2.235

Rizki, T.M., Rizki, R.M., Bellotti, R.A., 1985. Genetics of a *Drosophila* phenoloxidase. Molec. Gen. Genet. 201, 7–13. https://doi.org/10.1007/BF00397978

Salmand, P.-A., Iché-Torres, M., Perrin, L., 2011. Tissue-specific cell sorting from *Drosophila* embryos: Application to gene expression analysis. Fly (Austin) 5, 261–265. https://doi.org/10.4161/fly.5.3.16509

Schindelin, J., Arganda-Carreras, I., Frise, E., Kaynig, V., Longair, M., Pietzsch, T., Preibisch, S., Rueden, C., Saalfeld, S., Schmid, B., Tinevez, J.-Y., White, D.J., Hartenstein, V., Eliceiri, K., Tomancak, P., Cardona, A., 2012. Fiji: an open-source platform for biological-image analysis. Nat. Methods 9, 676–82. https://doi.org/10.1038/nmeth.2019

Shlyakhover, E., Shklyar, B., Hakim-Mishnaevski, K., Levy-Adam, F., Kurant, E., 2018. *Drosophila* GATA Factor Serpent Establishes Phagocytic Ability of Embryonic Macrophages. Front. Immunol. 9, 266. https://doi.org/10.3389/fimmu.2018.00266

Siekhaus, D., Haesemeyer, M., Moffitt, O., Lehmann, R., 2010. RhoL controls invasion and Rap1 localization during immune cell transmigration in *Drosophila*. Nat. Cell. Biol. 12, 605–610. https://doi.org/10.1038/ncb2063

Sonnenfeld, M.J., Jacobs, J.R., 1995. Macrophages and glia participate in the removal of apoptotic neurons from the *Drosophila* embryonic nervous system. J. Comp. Neurol. 359, 644–652. https://doi.org/10.1002/cne.903590410

Spahn, P., Huelsmann, S., Rehorn, K.-P., Mischke, S., Mayer, M., Casali, A., Reuter, R., 2014. Multiple regulatory safeguards confine the expression of the GATA factor Serpent to the hemocyte primordium within the *Drosophila* mesoderm. Dev. Biol. 386, 272–279. https://doi.org/10.1016/j.ydbio.2013.12.012

Stephenson, H.N., Streeck, R., Grüblinger, F., Goosmann, C., Herzig, A., 2022. Hemocytes are essential for *Drosophila melanogaster* post-embryonic development, independent of control of the microbiota. Development 149, dev200286. https://doi.org/10.1242/dev.200286

Tepass, U., Fessler, L.I., Aziz, A., Hartenstein, V., 1994. Embryonic origin of hemocytes and their relationship to cell death in *Drosophila*. Development 120, 1829–1837. https://doi.org/10.1242/dev.120.7.1829

Tokusumi, T., Tokusumi, Y., Schulz, R.A., 2018. The *mir-7* and *bag of marbles* genes regulate Hedgehog pathway signaling in blood cell progenitors in *Drosophila* larval lymph glands. Genesis 56, e23210. https://doi.org/10.1002/dvg.23210

Tokusumi, Y., Tokusumi, T., Stoller-Conrad, J., Schulz, R.A., 2010. Serpent, Suppressor of Hairless and U-shaped are crucial regulators of *hedgehog* niche expression and prohemocyte maintenance during *Drosophila* larval hematopoiesis. Development 137, 3561–3568. https://doi.org/10.1242/dev.053728

Vlisidou, I., Wood, W., 2015. *Drosophila* blood cells and their role in immune responses. FEBS J. 282, 1368–1382. https://doi.org/10.1111/febs.13235

Wang, L., Shalek, A.K., Lawrence, M., Ding, R., Gaublomme, J.T., Pochet, N., Stojanov, P., Sougnez, C., Shukla, S.A., Stevenson, K.E., Zhang, W., Wong, J., Sievers, Q.L., MacDonald, B.T., Vartanov, A.R., Goldstein, N.R., Neuberg, D., He, X., Lander, E., Hacohen, N., Regev, A., Getz, G., Brown, J.R., Park, H., Wu, C.J., 2014. Somatic mutation as a mechanism of Wnt/ -catenin pathway activation in CLL. Blood 124, 1089–1098. https://doi.org/10.1182/blood-2014-01-552067

Weavers, H., Evans, I.R., Martin, P., Wood, W., 2016. Corpse engulfment generates a molecular memory that primes the macrophage inflammatory response. Cell 165, 1658–1671. https://doi.org/10.1016/j.cell.2016.04.049

Yoon, S.-H., Cho, B., Lee, D., Kim, H., Shim, J., Nam, J.-W., 2023. Molecular traces of *Drosophila* hemocytes reveal transcriptomic conservation with vertebrate myeloid cells. PLoS Genet. 19, e1011077. https://doi.org/10.1371/journal.pgen.1011077

Yu, S., Luo, F., Xu, Y., Zhang, Y., Jin, L.H., 2022. *Drosophila* innate immunity involves multiple signaling pathways and coordinated communication between different tissues. Front. Immunol. 13, 905370. https://doi.org/10.3389/fimmu.2022.905370

Zettervall, C.-J., Anderl, I., Williams, M.J., Palmer, R., Kurucz, E., Ando, I., Hultmark, D., 2004. A directed screen for genes involved in *Drosophila* blood cell activation. Proc. Natl. Acad. Sci. U.S.A. 101, 14192–14197. https://doi.org/10.1073/pnas.0403789101